

# Premature Ignition: Why the Single-Degenerate Channel Leads to Type Iax and Not Type Ia Supernovae

Amir Michaelis<sup>1</sup> and Hagai B. Perets<sup>1</sup>

## Abstract

Type Ia supernovae (SNe Ia) are pivotal for the origins of the elements, the understanding of galactic chemical evolution, and serve as crucial cosmological distance indicators, yet their progenitor systems remain a central enigma in astrophysics. While both the growth of white dwarfs to near-Chandrasekhar mass and their explosion (the single-degenerate; SD) and mergers of two WDs leading to explosions (double-degenerate; DD) scenarios have been proposed, neither explains the observed diversity of thermonuclear transients and their properties, including the fainter Type Iax supernovae (SNe Iax). Here we show, through comprehensive three-dimensional hydrodynamic simulations, that as accreting WDs grow towards the Chandrasekhar mass (the SD channel), premature carbon ignition at sub-Chandrasekhar densities can trigger partial deflagrations that eject substantial mass in low-energy Iax outbursts. Such a process effectively serves as a self-limiting feedback loop, which stalls further mass growth. It naturally explains why the SD channel is precluded from producing standard, normal SNe Ia, and instead predominantly yields SNe Iax. Our findings significantly reframe the SD versus DD debate, with important implications for supernova rates, galactic chemical enrichment, and cosmological measurements.

## Introduction

Type Ia supernovae (SNe Ia) represent a fundamental class of stellar explosions with far-reaching implications for astrophysics. These thermonuclear events play crucial roles in galactic chemical evolution as primary producers of iron-peak elements Iwamoto et al. [1999], Seitzzahl et al. [2013], Palicio et al. [2023], influence the energy budget and dynamics of their host galaxies Taylor et al. [2014], Liang et al. [2024], Palicio et al. [2024], and serve as laboratories for extreme physics under degenerate conditions Hillebrandt et al. [2013]. Despite their importance across multiple domains of astrophysics, the nature of their progenitors and explosion mechanisms remains one of the most persistent open questions in stellar evolution theory.

Traditionally, progenitor models have been divided broadly into single-degenerate (SD) scenarios, where a carbon-oxygen (CO) white dwarf (WD) accretes mass from a non-degenerate companion, and double-degenerate (DD) scenarios involving the merger of two WDs [e.g. see reviews by Maoz et al., 2014, Soker, 2024, Ruitter and Seitzzahl, 2025]. Both scenarios face theoretical challenges in explaining the observed homogeneity and diversity of SNe Ia properties, timing of explosions, and nucleosynthetic yields.

Recent observational advances have revealed that thermonuclear supernovae exhibit considerably more diversity than the classical SNe Ia classification initially suggested Taubenberger [2017]. Modern transient surveys have identified numerous subclasses of thermonuclear events, including the extremely luminous "super-Chandrasekhar" events Howell et al. [2006], Scalzo et al. [2010], Phillips et al. [2024], the peculiar 2005E-like calcium-rich gap transients Perets et al. [2010], Kasliwal et al. [2012], the rapidly declining "SNe Ia-02es-like" objects Ganeshalingam et al. [2012], White et al. [2015], Cao et al. [2016], Bose et al. [2025], and the spectroscopically distinct "SNe Iax" Li et al. [2003], Foley et al. [2013]. This diversity challenges our understanding of thermonuclear explosion mechanisms and the evolutionary pathways leading to them.

Among these peculiar transients, Type Iax supernovae (SNe Iax) constitute a prominent subclass, initially identified with SN 2002cx Li et al. [2003], Foley et al. [2013]. Unlike classical SNe Ia, SNe Iax exhibit lower peak luminosities, lower ejecta velocities (approximately 2,000–8,000 km s<sup>-1</sup>), asymmetric ejecta, and smaller <sup>56</sup>Ni yields ranging from 0.03 to 0.2  $M_{\odot}$  Foley et al. [2013], Jha [2017]. Moreover, SNe Iax spectra show persistent low-ionization features at late phases, indicative of incomplete burning and suggesting a partially exploded remnant WD Sahu et al. [2008], Jha et al. [2006], Foley et al. [2016], Camacho-Neves et al. [2023], Schwab et al. [2025].

Earlier theoretical work has demonstrated that partial deflagration explosions of near-Chandrasekhar-mass CO WDs can naturally produce observed SN Iax characteristics, including moderate ejecta velocities, modest nickel yields, and remnant natal kicks due to asymmetric ejection Jordan et al. [2012], Kromer et al. [2013], Fink et al.

[2014], Mehta et al. [2024]. Specifically, Jordan et al. [2012] suggested that incomplete deflagration of near-Chandrasekhar mass WDs leads to asymmetric ejecta, natal kicks to surviving WD remnants, and lower yields of radioactive  $^{56}\text{Ni}$ . Nevertheless, this scenario raises the critical unresolved question of why some CO WDs experience only partial deflagration, resulting in Type Iax, whereas others undergo complete deflagration, transitioning into detonation, producing normal SNe Ia. A related challenge in SD models involves the limitations on WD growth due to nova eruptions. As WDs accrete material from their companions, periodic nova explosions can expel accreted matter, potentially halting the WD growth towards the Chandrasekhar limit Iben and Tutukov [1984], Yaron et al. [2005], Starrfield et al. [2020], Hillman [2021], Hillman et al. [2025].

Analogous to the nova-eruptions limiting challenge, we propose that a similar limiting phenomenon occurs not only via surface novae but also through internal deflagration ignition processes. In particular, CO WDs may ignite prematurely at sub-Chandrasekhar masses, initiating partial deflagrations that fail to transition to full detonation. Such early ignition, triggered by lower central densities, may preferentially yield Type Iax events rather than classical SNe Ia, and will expel significant mass, not allowing for further growth of the WD and precluding a full normal type Ia SNe from this channel. In this study, we employ detailed three-dimensional hydrodynamic simulations to explore the deflagration mechanism in single-degenerate sub-Chandrasekhar CO WDs. We systematically vary WD masses and ignition conditions to determine the circumstances under which partial deflagrations, rather than full detonations, occur. Our results demonstrate that ignition at lower WD masses consistently produces explosion signatures consistent with the observational properties of SNe Iax, thereby offering theoretical support for the hypothesis of premature ignition as a critical pathway to these peculiar explosions. This insight provides a coherent explanation for the diversity observed among thermonuclear supernovae and the population of sub-Chandrasekhar WDs that never reach full detonation but rather manifest observationally as SNe Iax. Our findings indicate that premature ignition at sub-Chandrasekhar masses imposes a significant constraint on the single-degenerate scenario, suggesting it rarely leads to typical Type Ia SNe.

## Results

Our three-dimensional hydrodynamic simulations (see Fig. 1 and methods section) reveal a clear mass-dependent transition in the explosion outcomes of ignited white dwarfs. For WDs with masses  $\lesssim 1.365 M_{\odot}$ , we con-

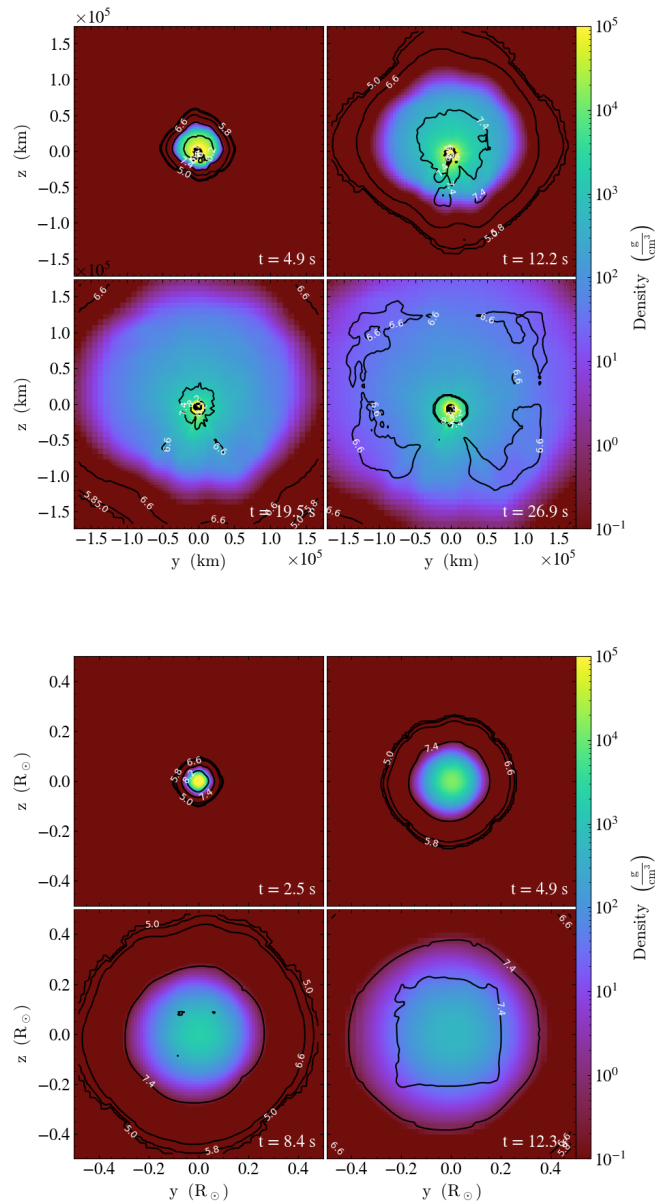


Figure 1: **Time evolution of the deflagration front and density structure for representative models.** **Top row:**  $1.330 M_{\odot}$  WD (partial deflagration). Snapshots are shown at 2.5 and 4.9 seconds. **Bottom row:**  $1.374 M_{\odot}$  WD (complete disruption). Snapshots are shown at 8.4 and 12.3 seconds. The color map changes from red ( $0.1 \text{ g cm}^{-3}$ ) up to yellow ( $10^5 \text{ g cm}^{-3}$ ). The contours represent the temperature at 5 different values. The asymmetric burning in the partial deflagration case contrasts with the nearly symmetric energy release in the complete disruption case.

sistently observe partial deflagrations that fail to unbind the entire star. These incomplete explosions leave behind a remnant WD, typically ejecting  $0.1 - 0.5 M_{\odot}$  of material with characteristic velocities of  $3,000 - 5,000 \text{ km s}^{-1}$  and producing modest amounts of  $^{56}\text{Ni}$  ( $0.03 - 0.09 M_{\odot}$ ). In contrast, WDs with masses  $\gtrsim 1.370 M_{\odot}$  undergo complete disruption, with no remaining bound remnant (see Fig. 2). These energetic explosions produce significantly higher nickel yields ( $0.5 - 1.2 M_{\odot}$ ; Fig. 3) and eject material at much higher velocities ( $8,000 - 10,000 \text{ km s}^{-1}$ ; Fig. 4). The transition between these two regimes occurs over a remarkably narrow mass range of approximately  $0.005 M_{\odot}$ . The relationship between the mass of the white dwarf and the unbounded mass ejected (Figure 2) and the  $^{56}\text{Ni}$  yield (Figure 3) clearly illustrate this sharp transition in nickel production at approximately  $1.370 M_{\odot}$ . The ejected mass and the velocity show a much more moderate dependency on the initial WD mass for partial deflagrations (Figure 4).

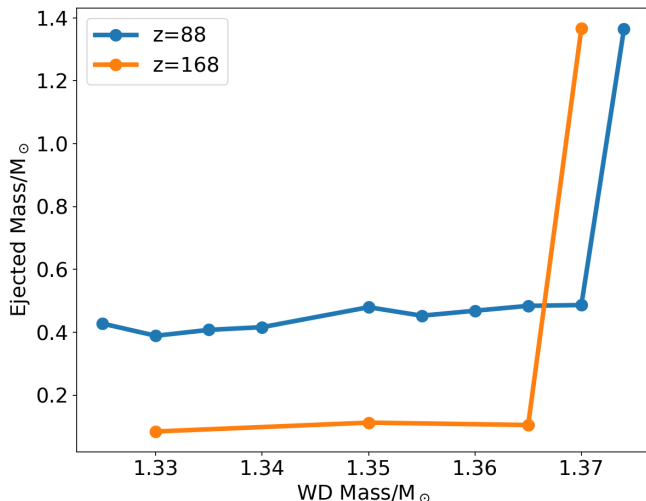


Figure 2: **Relationship between white dwarf mass and ejected mass.** The blue line represents models with an ignition offset of 88 km, while the orange line represents models with an ignition offset of 168 km. Note the sharp transition in ejected material at approximately  $1.370 M_{\odot}$ , corresponding to the boundary between partial deflagrations and complete disruptions. There is a strong dependency of the ejected material on the ignition offset; for a given offset, we see a much more subtle change in the ejected mass.

Our simulations also demonstrate significant sensitivity to the ignition geometry, particularly the offset distance of the ignition region from the WD center. As shown in Table 1, models with an ignition offset of 168 km consistently

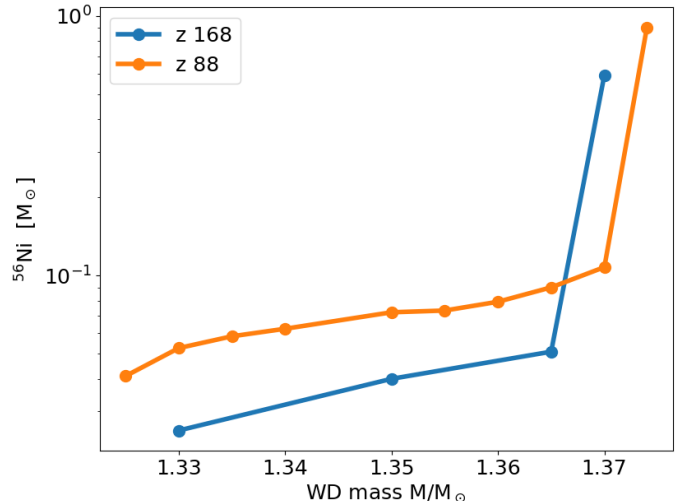


Figure 3: **Relationship between white dwarf mass and  $^{56}\text{Ni}$  yield.** The blue line represents models with an ignition offset of 88 km, while the orange line represents models with an ignition offset of 168 km. Note the sharp transition in nickel production at approximately  $1.370 M_{\odot}$ , corresponding to the boundary between partial deflagrations and complete disruptions. A clear dependency between the nickel yield from the explosion and the initial WD mass is evident.

tently produce weaker explosions compared to their counterparts with an ignition offset of 88 km, for the same WD mass. For instance, model w1350-z168 ejects only  $0.113 M_{\odot}$  with  $0.040 M_{\odot}$  of  $^{56}\text{Ni}$ , whereas model w1350-z88 ejects  $0.480 M_{\odot}$  with  $0.072 M_{\odot}$  of  $^{56}\text{Ni}$ . This difference is particularly pronounced for intermediate-mass WDs ( $1.350 - 1.365 M_{\odot}$ ), where the ignition offset can determine whether the explosion ejects a significant fraction of the WD mass or only a small outer layer. Interestingly, for the highest-mass WDs in our study ( $1.370 M_{\odot}$  and above), the ignition offset primarily affects the energy distribution and nucleosynthetic yields rather than the overall explosion outcome. Both models w1370-z88 and w1370-z168 lead to complete disruption of the WD, although with different  $^{56}\text{Ni}$  yields ( $0.108$  vs.  $0.593 M_{\odot}$ ). This suggests that while the ignition geometry modulates the explosion strength, the WD mass ultimately determines whether the star undergoes complete disruption.

The explosion dynamics of our simulated WDs exhibit distinctive characteristics based on mass. In lower-mass WDs, the deflagration front propagates asymmetrically through the star, burning only a fraction of the available fuel before the expansion of the star quenches the flame. This asymmetric burning results in asymmetric

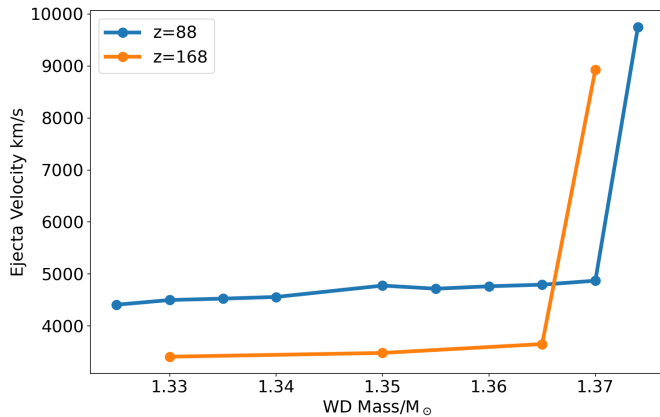


Figure 4: **Relationship between the WD mass and ejected mass velocity.** The blue line represents ignition points centered at  $z = 88$  km, and the yellow line represents the center at  $z = 168$  km. The destroyed WDs (models w1374-z88 and w1370-z168) show velocities typical of Type Ia supernovae ( $\sim 10,000$  km  $s^{-1}$ ). The partially exploded WDs have typical velocities of Type Iax supernovae, slowly ranging between  $4000 - 5000$  km  $s^{-1}$ .

ejecta and imparts a natal kick to the remnant WD in the direction opposite to the primary ejecta. Our simulations yield kick velocities ranging from  $100$  to  $500$  km  $s^{-1}$ , with higher kicks generally associated with larger ejecta masses (see Figure 5). The surviving remnants from partial deflagrations typically have masses of  $0.9 - 1.2 M_{\odot}$  and significantly expanded radii compared to their pre-explosion state. These remnants are heated by deflagration and show strong convective mixing, leaving them with a unique composition profile that includes partially burned material and ash from nuclear burning. In contrast, the highest-mass WDs in our study develop a more symmetric and energetic burning front that transitions to a detonation wave, consuming the entire star and leaving no bound remnant. The transition from deflagration to detonation occurs when the deflagration front reaches regions of critical density and temperature conditions, typically in the range of  $1 - 2 \times 10^9$  g  $cm^{-3}$ . Figure 1 illustrates the time evolution of the deflagration front and density structure for representative models of each mass regime.

The nucleosynthetic yields from our simulations provide further insights into the explosion mechanisms and their observational signatures. For partial deflagrations (lower-mass WDs), the composition of the ejecta is dominated by intermediate-mass elements (IMEs) such as silicon, sulfur, and calcium, with relatively small amounts of iron-group elements. The  $^{56}\text{Ni}$  fraction in these models typically constitutes  $10 - 20\%$  of the mass of the ejecta. This composition is consistent with the observed spectra

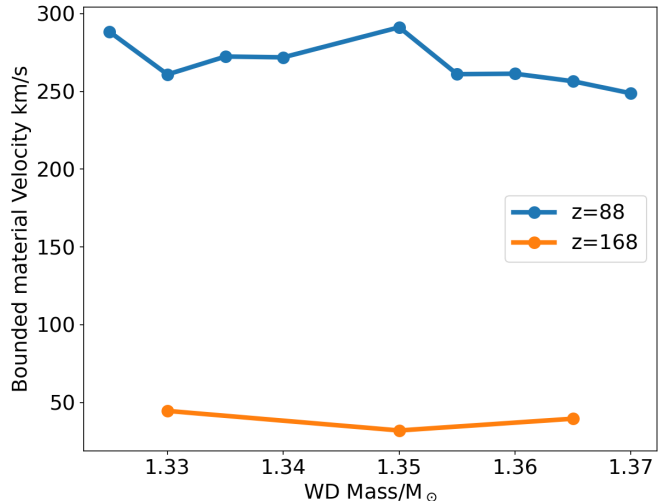


Figure 5: **Relationship between the WD mass and the kick velocity of the bounded material.** The blue line represents ignition points centered at  $z = 88$  km and the yellow line represents the center at  $z = 168$  km. The destroyed WDs (models w1374-z88 and w1370-z168) are omitted from this plot as there is no kick velocity in these cases.

of SNe Iax, which show strong IME features and relatively weak iron-group signatures at early times. In contrast, the complete disruption models (higher-mass WDs) produce ejecta rich in iron-group elements, with  $^{56}\text{Ni}$  accounting for  $40 - 60\%$  of the ejecta mass. This composition aligns well with normal SNe Ia, which exhibit strong iron-group element features in their spectra. The sharp transition in nucleosynthetic yields observed across our mass sequence provides a natural explanation for the distinct observational properties of SNe Iax versus normal SNe Ia, with the WD mass at ignition being the primary determining factor. Figure 6 presents the  $^{56}\text{Ni}$  yield against ejecta velocity for the different models.

## Discussion

Our simulation results offer a compelling explanation for the observed characteristics of Type Iax supernovae. The partial deflagrations of sub-Chandrasekhar mass WDs consistently produce explosions with ejecta velocities,  $^{56}\text{Ni}$  yields, and total ejected masses that align remarkably well with observed SNe Iax properties Foley et al. [2013], Jha [2017], Srivastav et al. [2022]. Our simulated ejecta velocities ( $3,000 - 5,000$  km  $s^{-1}$ ) fall squarely within the range of observed photospheric velocities in SNe Iax ( $2,000 - 8,000$  km  $s^{-1}$ ). Similarly, our  $^{56}\text{Ni}$  yields

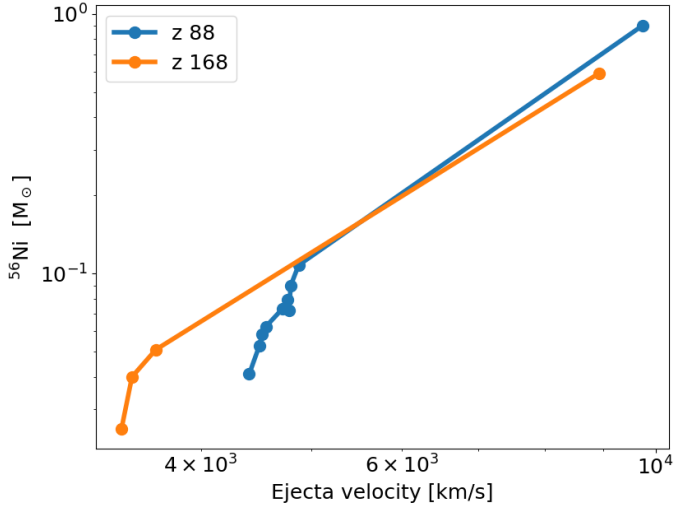


Figure 6:  $^{56}\text{Ni}$  ejecta for selected models. A log-log plot of nickel in units of solar mass against the velocity of the nickel shell ejecta in units of  $\text{km s}^{-1}$ . The blue line represents ignition points centered at  $z = 88$  km, and the yellow line represents the center at  $z = 168$  km. The destroyed WDs (models w1374-z88 and w1370-z168) show nickel and velocities typical of Type Ia SN. The partially exploded WDs have typical nickel and velocities of type Iax SNe.

( $0.03 - 0.1 M_{\odot}$ ) match the inferred radioactive yields of observed events, which typically range from  $0.03$  to  $0.2 M_{\odot}$ . Figure 7 directly compares our model predictions with observed SNe Iax properties. The heterogeneity within the SNe Iax class can be naturally explained within our framework by variations in the WD mass and ignition conditions. We should note that 2008ha-like fainter SNe (e.g., Foley et al. [2009], Stritzinger et al. [2014]) were not produced by our models. It is possible that events like SN 2008ha and SN 2010ae, with inferred  $^{56}\text{Ni}$  masses of only  $\sim 0.003 M_{\odot}$ , could result from ignitions occurring at even lower WD masses or more extreme offsets than those explored in our current parameter study. Alternatively, while 2008ha-like SNe were suggested to be an integral part of the Iax SNe Foley et al. [2013], including both brighter 2002cx-like SNe and fainter 2008ha-like SNe, observations do show a clear luminosity gap between brighter and fainter Iax SNe, raising the possibility that they result from different channels. Hence, not obtaining very faint SNe in our models might be consistent with such a possibility of two distinct channels, and may support it. On the brighter side of Iax SNe, the relatively luminous SN 2012Z Yamanaka et al. [2015], with an estimated  $^{56}\text{Ni}$  mass of  $\sim 0.18 M_{\odot}$ , might represent

an explosion of a WD near the upper mass boundary of the partial deflagration regime. The persistent detection of bound remnants in our simulations aligns with late-time observations of SNe Iax, which often show peculiar spectroscopic features inconsistent with complete disruption scenarios Jha et al. [2006], Foley et al. [2016]. These remnants could potentially be observed as unusual WDs with peculiar atmospheric compositions, high velocities, and inflated radii, and were possibly observed, e.g. Ref. Vennes et al. [2017].

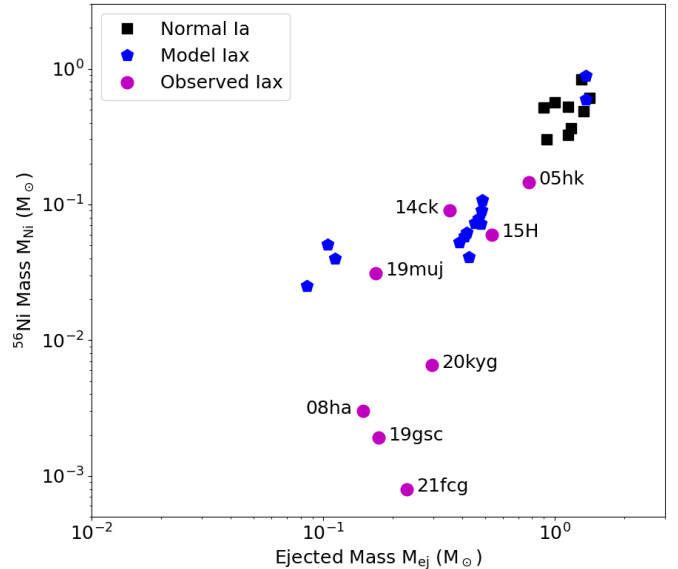


Figure 7: **Comparison between our simulation results and observed properties of SNe Iax.** Our simulation results (marker with blue pentagons) are compared with observed SNe Iax properties (mark with magenta circles). Normal type Ia (marked with black squares) are added for perspective. The vertical axis shows the  $^{56}\text{Ni}$  mass yield, while the horizontal axis shows the ejected mass. The observed properties are from Srivastav et al. [2022] figure 16. Our partial deflagration models populate the same region of parameter space as observed SNe Iax, while our complete disruption models align with normal SNe Ia.

Our finding that WDs with masses below  $\sim 1.370 M_{\odot}$  consistently undergo partial rather than complete explosions has major implications for single-degenerate evolution scenarios. This result suggests that the majority of accreting WDs in single-degenerate systems may never reach the conditions necessary for normal Type Ia explosions. In traditional single-degenerate scenarios, a CO WD accretes hydrogen-rich material from a non-degenerate companion, growing toward the Chan-

drasekhar limit Nomoto [1982], Hachisu et al. [1996]. However, this growth process faces several theoretical challenges, including nova eruptions that may expel more mass than is accreted Yaron et al. [2005], Hillman et al. [2016]. Our work introduces an additional, potentially more fundamental limitation: even if a WD successfully accretes enough material to reach masses of  $1.32 - 1.37 M_{\odot}$ , it becomes increasingly susceptible to premature ignition, leading to a partial deflagration. This premature ignition scenario resembles a "safety valve" in single-degenerate evolution: as the WD's mass increases and its central density rises, the probability of spontaneous carbon ignition grows dramatically. Once ignited, the partial deflagration ejects a substantial fraction of the accreted mass, effectively resetting the growth process. In principle, this cycle could repeat multiple times during a binary's evolution, with each partial explosion manifesting as a SNe Iax, however, the original mass-growth towards a near-Chandrasekhar mass WD already exhausts much of the potential mass to be created from a companion, and any additional accretion might not allow for sufficient growth towards another explosion. The WD-kicks may also change the later evolution of the remnant binary. These, however, do not preclude a merger of the companion donor star remnant, once it becomes a WD with the current WD accretor, which then potentially follows a double-degenerate channel for type Ia SN, i.e. the same system could produce more than one SN, one for an SD channel and later from a DD channel.

The sharp transition in explosion outcome that we observe near  $1.370 M_{\odot}$  provides important physical insight into the deflagration-to-detonation transition (DDT) process. Our simulations suggest that at this critical mass threshold, the central density reaches values where the deflagration burning becomes sufficiently energetic and the nuclear timescales become competitive with the hydrodynamic expansion timescales, allowing a transition to detonation. The existence of this threshold explains why SNe Iax and normal SNe Ia appear as distinct populations rather than forming a continuous spectrum of explosion properties. The threshold behavior creates a natural bifurcation in outcomes: WDs below the threshold produce SNe Iax, while those above it yield normal SNe Ia. However, this threshold is not solely determined by mass. As our results show, ignition geometry also plays a crucial role, particularly at masses near the transition point. The strong dependence on ignition conditions at masses around  $1.365 - 1.370 M_{\odot}$  introduces an element of stochasticity in explosion outcomes, which could explain some of the observed diversity within both the SNe Iax and normal SNe Ia populations.

Our model makes several testable predictions for future observations. First, if most single-degenerate WDs undergo premature ignition as we propose, then SNe Iax

should occur at rates comparable to or higher than normal SNe Ia from this channel. Theoretical rate estimates for the SD channel typically suggest 10 – 15% of the current observational inferred type Ia rates. Current observational estimates suggest that SNe Iax represent approximately 5 – 30% of the total SN Ia rate Foley et al. [2013], Miller et al. [2017], which is consistent with our scenario where type Iax SNe are effectively the outcomes of the SD channel rather than normal Ia SNe. Second, our model predicts a strong positive correlation between ejecta mass, nickel yield, and expansion velocity within the SNe Iax class, driven primarily by variations in the progenitor WD mass. These are generally consistent with current observations [see also Foley et al., 2013]. Future high-cadence surveys with instruments like the Vera C. Rubin Observatory will enable more systematic characterization of SNe Iax properties, allowing this prediction to be tested across a larger sample. Third, we support previous predictions Jordan et al. [2012] of the existence of a population of kicked WD remnants with unusual compositions and thermal properties. These objects would appear as peculiar WDs with atmospheres contaminated by deflagration ash, moderately high velocities ( $100 - 500 \text{ km s}^{-1}$ ), and potentially inflated radii. Dedicated searches for such objects in our galactic neighborhood could provide direct confirmation of the partial deflagration scenario. In particular, current observations of peculiar hypervelocity WDs at hundreds of  $\text{km s}^{-1}$  [e.g., Vennes et al., 2017], may have already identified such remnants. Finally, if premature ignition is indeed common, we would expect a relative scarcity of super-Chandrasekhar or near-Chandrasekhar mass CO WDs in accreting binary systems, as these objects would be vulnerable to ignition before reaching such high masses. Demographic studies of WD masses in close binaries could test this prediction.

## Summary and Conclusions

Our three-dimensional hydrodynamic simulations reveal that the ignition of sub-Chandrasekhar mass carbon-oxygen white dwarfs (CO WDs) in single-degenerate systems naturally produces partial deflagrations with properties that closely match observed Type Iax supernovae. These simulations demonstrate a sharp transition in explosion outcomes at approximately  $1.370 M_{\odot}$ : lower-mass WDs consistently undergo incomplete deflagrations that leave behind remnants, while higher-mass WDs experience complete disruption characteristic of normal Type Ia supernovae.

The partial deflagration outcomes reproduce key observational signatures of Type Iax events, including:

- Moderate ejecta velocities ( $3,000 - 5,000 \text{ km s}^{-1}$ )
- Modest  $^{56}\text{Ni}$  yields ( $0.03 - 0.1 M_{\odot}$ )

- Substantial bound remnants ( $0.9 - 1.2 M_{\odot}$ )
- Asymmetric ejecta distributions

Our results suggest that the intrinsic diversity observed among Type Iax supernovae likely stems from variations in both WD mass and ignition conditions, with more off-set ignitions generally producing weaker explosions compared to central ignitions at the same WD mass.

Critically, our findings indicate that premature ignition represents a fundamental limiting mechanism in the evolution of accreting WDs, analogous to but distinct from the constraints imposed by classical nova eruptions. This "safety valve" mechanism effectively interrupts the growth of WDs toward the Chandrasekhar limit, as WDs reaching masses of  $1.32 - 1.37 M_{\odot}$  become increasingly susceptible to carbon ignition that results in partial deflagrations rather than complete detonations.

This has profound implications for supernova progenitor theory: the single-degenerate channel may predominantly produce Type Iax supernovae rather than normal Type Ia events. This constraint helps explain several observational puzzles, including the relative rates of Type Iax and Type Ia supernovae, and suggests that alternative progenitor scenarios—such as double-degenerate mergers or sub-Chandrasekhar double detonations—may be required to account for normal Type Ia supernovae.

Our model makes several testable predictions for future observations:

1. A strong positive correlation between ejecta mass, nickel yield, and expansion velocity within the Type Iax class.
2. The existence of a population of kicked WD remnants with unusual compositions, moderate velocities ( $100 - 500 \text{ km s}^{-1}$ ), and potentially inflated radii.
3. A relative scarcity of super-Chandrasekhar or near-Chandrasekhar mass WDs in accreting binary systems.

The mass threshold we identify (approximately  $1.370 M_{\odot}$ ) provides important physical insight into the deflagration-to-detonation transition process and explains why Type Iax and normal Type Ia supernovae appear as distinct populations rather than forming a continuous spectrum of explosion properties.

Future work should focus on refining our understanding of ignition conditions in accreting WDs, exploring a wider range of ignition geometries and compositions, and developing more sophisticated nucleosynthesis calculations to enable direct comparison with observed spectra. Additionally, incorporating these findings into binary population synthesis models will be crucial for predicting the relative rates of different thermonuclear transients and

assessing the overall contribution of the single-degenerate channel to the supernova population.

Our results significantly constrain the viability of the single-degenerate channel as a pathway toward classical Type Ia explosions, suggesting that the diversity of thermonuclear supernovae reflects not only variations in explosion mechanisms but also fundamental differences in progenitor evolution. This framework provides a coherent explanation for the observed diversity of thermonuclear transients and highlights the critical role of understanding sub-Chandrasekhar ignition processes in the broader context of stellar evolution and galactic chemical enrichment.

## Methods

### Hydrodynamic Simulations

We conducted comprehensive three-dimensional hydrodynamic simulations using the adaptive-mesh refinement (AMR) code FLASH version 4.7 Fryxell et al. [2000]. FLASH is particularly well-suited for modeling thermonuclear explosions due to its modular architecture, robust AMR capabilities, and specialized physics modules for nuclear burning and degenerate matter.

For all simulations, we employed the directionally unsplit hydrodynamic solver Lee [2006], Lee and Deane [2009], Lee [2013], which accurately captures three-dimensional shock propagation and complex flow patterns essential for modeling deflagration fronts. The degenerate matter was described using the Helmholtz equation of state Aparicio [1998], Timmes and Arnett [1999], Timmes and Swesty [2000], which incorporates electron degeneracy pressure, Coulomb corrections, radiation pressure, and thermal contributions from ions—all critical components for accurately modeling WD interiors across a wide range of densities and temperatures.

To simulate nuclear burning processes, we implemented the reaction-advection-diffusion flame model developed by Calder et al. [2007] and Townsley et al. [2007, 2009, 2016]<sup>1</sup>. This model tracks the propagation of the thermonuclear flame front through the degenerate material using an advection-diffusion-reaction equation approach, capturing both the subsonic deflagration phase and potential transitions to detonation. The nuclear reaction network follows the major energy-producing reactions including carbon, oxygen, and helium burning channels, accurately accounting for the energy release and nuclear statistical equilibrium (NSE) conditions reached in the densest regions.

<sup>1</sup><https://pages.astronomy.ua.edu/townsley/code/>

## Initial Models and Simulation Setup

We constructed a series of hydrostatic CO WD models with masses ranging from  $1.325$  to  $1.374 M_{\odot}$ , corresponding to central densities between  $4.8 \times 10^8$  and  $1.2 \times 10^9 \text{ g cm}^{-3}$ . Each initial model was generated by numerically integrating the hydrostatic equilibrium equation using the Helmholtz EOS with a uniform initial temperature of  $10^7 \text{ K}$  and a uniform 50/50 carbon-oxygen composition by mass.

These WD models were mapped onto the three-dimensional FLASH grid and allowed to relax over several dynamical timescales to ensure hydrostatic equilibrium before ignition. Our computational domain spanned  $(1 \times 10^{11} \text{ cm})^3$  with 15 levels of refinement, providing an effective resolution of 7.63 km at the highest refinement level. This resolution is sufficient to capture the propagation and development of the deflagration fronts while remaining computationally feasible for a systematic parameter study.

To initiate the deflagration process, we used a stochastic multi-point ignition scenario. Specifically, we positioned 63 ignition points randomly within a spherical shell of radius 128 km, centered at two different offset positions along the  $z$ -axis:  $z = 88 \text{ km}$  and  $z = 168 \text{ km}$  from the WD center. Each ignition kernel was modeled as a spherical region of radius 16 km with fully burned material ("ash") at an elevated temperature corresponding to the energy release from carbon fusion (Figure 8). This multi-point ignition setup allows us to systematically investigate how the asymmetry and geometry of the initial burning region affect the overall explosion dynamics.

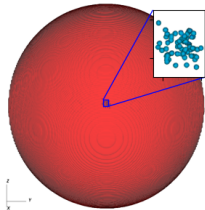


Figure 8: **Initial Ignition Setup.** The red sphere represents the white dwarf (WD). The inner region indicates the initial deflagration zone. A zoomed-in view of this region is shown in the upper right corner. The blue spheres represent the ignited ("ash") points. These are confined within a sphere of 128 km radius, centered at either  $z = 88 \text{ km}$  or  $z = 168 \text{ km}$ . Each point has a radius of 16 km, and there are a total of 63 such points spread randomly inside the confined region.

Table 1 summarizes the key parameters for all simulation models in our study, including the WD masses, cen-

tral densities, ignition configurations, and resulting explosion properties. For each model, we tracked the simulation until either the deflagration fully consumed the WD or the partial burning phase reached a quasi-steady state (typically 2-3 seconds of physical time), after which we analyzed the ejecta properties, nucleosynthetic yields, and remnant characteristics.

## Analysis Methods

To analyze the simulation results, we tracked multiple explosion metrics throughout each simulation. These included the mass of synthesized radioactive  $^{56}\text{Ni}$ , total ejected mass, remnant mass (if any), characteristic ejecta velocities, and explosion energy. The ejecta was defined as material with positive total energy (kinetic plus potential plus internal), while bound material was considered part of the remnant.

For each model, we calculated the mass-weighted mean radial velocity of the ejecta to characterize the typical expansion speeds. We also tracked the morphology of the deflagration front to identify whether the burning remained asymmetric (leading to partial deflagration) or encompassed the entire star (leading to complete disruption). The asymmetry of the ejecta was quantified using the center-of-mass offset from the initial WD center, allowing us to estimate the resulting kick velocities of any remnants. We calculate the nucleosynthesis in post-processing using a 136-isotope network and between 350,000 and 500,000 Lagrangian particles.

We performed these simulations on the Technion Nyx high-performance computer using 576 CPU cores per simulation, with typical run times of approximately 414,720 CPU hours per model.

## Data Availability

The datasets generated and analyzed during the current study will be made available upon reasonable request to the corresponding author.

## Code Availability

The FLASH code is an open-source, publicly available multiphysics simulation code (<https://flash.uchicago.edu/>). Specific modifications and input files used for these simulations can be made available upon reasonable request.

## Acknowledgements

We acknowledge support for this project from the European Union's Horizon 2020 research and innovation pro-

Table 1: **Summary of Simulation Parameters and Outcomes.** The columns show: model designation, ignition offset along the  $z$ -axis (km), WD mass ( $M_{\odot}$ ), central density ( $10^9 \text{ g cm}^{-3}$ ), ejecta mass ( $M_{\odot}$ ), characteristic ejecta velocity ( $\text{km s}^{-1}$ ), and synthesized  $^{56}\text{Ni}$  mass ( $M_{\odot}$ ). Models w1374-z88 and w1370-z168 are the only models to achieve full detonation and no bounded mass remains.

Model name	Offset (km)	Mass ( $M_{\odot}$ )	$\rho_c$ ( $10^9 \text{ g cm}^{-3}$ )	$M_{\text{ej}}$ ( $M_{\odot}$ )	$V_{\text{ej}}$ ( $\text{km s}^{-1}$ )	$^{56}\text{Ni}$ ( $M_{\odot}$ )
w1325-z88	88	1.325	0.488	0.428	4410	0.041
w1330-z88	88	1.330	0.518	0.389	4499	0.053
w1335-z88	88	1.335	0.568	0.408	4527	0.058
w1340-z88	88	1.340	0.608	0.417	4559	0.062
w1350-z88	88	1.350	0.728	0.480	4777	0.072
w1355-z88	88	1.355	0.788	0.453	4717	0.073
w1360-z88	88	1.360	0.868	0.469	4764	0.079
w1365-z88	88	1.365	0.958	0.484	4795	0.090
w1370-z88	88	1.370	1.190	0.487	4871	0.108
w1374-z88	88	1.374	1.290	1.364	9751	0.893
w1330-z168	168	1.330	0.518	0.085	3409	0.025
w1350-z168	168	1.350	0.728	0.113	3483	0.040
w1365-z168	168	1.365	0.958	0.105	3653	0.051
w1370-z168	168	1.370	1.190	1.367	8933	0.593

gram under grant agreement No 865932-ERC-SNeX.

## References

- Koichi Iwamoto, Franziska Brachwitz, Ken’ICHI Nomoto, Nobuhiro Kishimoto, Hideyuki Umeda, W. Raphael Hix, and Friedrich-Karl Thielemann. Nucleosynthesis in Chandrasekhar Mass Models for Type IA Supernovae and Constraints on Progenitor Systems and Burning-Front Propagation. *ApJS*, 125(2):439–462, December 1999. doi: 10.1086/313278.
- Ivo R. Seitenzahl, Franco Ciaraldi-Schoolmann, Friedrich K. Röpke, Michael Fink, Wolfgang Hillebrandt, Markus Kromer, Rüdiger Pakmor, Ashley J. Ruiter, Stuart A. Sim, and Stefan Taubenberger. Three-dimensional delayed-detonation models with nucleosynthesis for Type Ia supernovae. *MNRAS*, 429(2): 1156–1172, February 2013. doi: 10.1093/mnras/sts402.
- P. A. Palicio, E. Spitoni, A. Recio-Blanco, F. Matteucci, S. Peirani, and L. Greggio. Analytic solution of chemical evolution models with Type Ia supernovae. I. Disc bimodality in the  $[\alpha/\text{Fe}]$  versus  $[\text{Fe}/\text{H}]$  plane and other applications. *A&A*, 678:A61, October 2023. doi: 10.1051/0004-6361/202346567.
- Matt Taylor, David Cinabro, Ben Dilday, Lluís Galbany, Ravi R. Gupta, R. Kessler, John Marriner, Robert C. Nichol, Michael Richmond, Donald P. Schneider, and Jesper Sollerman. The Core Collapse Supernova Rate from the SDSS-II Supernova Survey. *ApJ*, 792(2):135, September 2014. doi: 10.1088/0004-637X/792/2/135.
- Zhuoxi Liang, Nao Suzuki, Mamoru Doi, Masayuki Tanaka, and Naoki Yasuda. Luminosity Functions of the Host Galaxies of Supernova. *ApJ*, 970(1):52, July 2024. doi: 10.3847/1538-4357/ad4b19.
- P. A. Palicio, F. Matteucci, M. Della Valle, and E. Spitoni. Cosmic Type Ia supernova rate and constraints on supernova Ia progenitors. *A&A*, 689:A203, September 2024. doi: 10.1051/0004-6361/202449740.
- W. Hillebrandt, M. Kromer, F. K. Röpke, and A. J. Ruiter. Towards an understanding of Type Ia supernovae from a synthesis of theory and observations. *Frontiers of Physics*, 8(2):116–143, April 2013. doi: 10.1007/s11467-013-0303-2.
- Dan Maoz, Filippo Mannucci, and Gijs Nelemans. Observational Clues to the Progenitors of Type Ia Supernovae. *ARA&A*, 52:107–170, August 2014. doi: 10.1146/annurev-astro-082812-141031.
- Noam Soker. Supernovae in 2023 (review): possible breakthroughs by late observations. *The Open Journal of Astrophysics*, 7:31, April 2024. doi: 10.33232/001c.117147.
- Ashley Jade Ruiter and Ivo Rolf Seitenzahl. Type Ia supernova progenitors: a contemporary view of a long-standing puzzle. *A&A Rev.*, 33(1):1, December 2025. doi: 10.1007/s00159-024-00158-9.
- Stefan Taubenberger. The Extremes of Thermonuclear Supernovae. In Athem W. Alsabti and Paul Murdin, editors, *Handbook of Supernovae*, page 317. 2017. doi: 10.1007/978-3-319-21846-5-37.

- D. Andrew Howell, Mark Sullivan, Peter E. Nugent, Richard S. Ellis, Alexander J. Conley, Damien Le Borgne, Raymond G. Carlberg, Julien Guy, David Balam, Stephane Basa, Dominique Fouchez, Isobel M. Hook, Eric Y. Hsiao, James D. Neill, Reynald Pain, Kathryn M. Perrett, and Christopher J. Pritchett. The type Ia supernova SNLS-03D3bb from a super-Chandrasekhar-mass white dwarf star. *Nature*, 443(7109):308–311, September 2006. doi: 10.1038/nature05103.
- R. A. Scalzo, G. Aldering, P. Antilogus, C. Aragon, S. Bailey, C. Baltay, S. Bongard, C. Buton, M. Childress, N. Chotard, Y. Copin, H. K. Fakhouri, A. Gal-Yam, E. Gangler, S. Hoyer, M. Kasliwal, S. Loken, P. Nugent, R. Pain, E. Pécontal, R. Pereira, S. Perlmutter, D. Rabinowitz, A. Rau, G. Rigaudier, K. Runge, G. Smadja, C. Tao, R. C. Thomas, B. Weaver, and C. Wu. Nearby Supernova Factory Observations of SN 2007if: First Total Mass Measurement of a Super-Chandrasekhar-Mass Progenitor. *ApJ*, 713(2):1073–1094, April 2010. doi: 10.1088/0004-637X/713/2/1073.
- M. M. Phillips, C. Ashall, Peter J. Brown, L. Galbany, M. A. Tucker, Christopher R. Burns, Carlos Contreras, P. Hoefflich, E. Y. Hsiao, S. Kumar, Nidia Morrell, Syed A. Uddin, E. Baron, Wendy L. Freedman, Kevin Krisciunas, S. E. Persson, Anthony L. Piro, B. J. Shappee, Maximilian Stritzinger, Nicholas B. Suntzeff, Sudeshna Chakraborty, R. P. Kirshner, J. Lu, G. H. Marion, Abigail Polin, and M. Shahbandeh. 1991T-like Supernovae. *ApJS*, 273(1):16, July 2024. doi: 10.3847/1538-4365/ad4f7e.
- H. B. Perets, A. Gal-Yam, P. A. Mazzali, D. Arnett, D. Kagan, A. V. Filippenko, W. Li, I. Arcavi, S. B. Cenko, D. B. Fox, D. C. Leonard, D. S. Moon, D. J. Sand, A. M. Soderberg, J. P. Anderson, P. A. James, R. J. Foley, M. Ganeshalingam, E. O. Ofek, L. Bildsten, G. Nelemans, K. J. Shen, N. N. Weinberg, B. D. Metzger, A. L. Piro, E. Quataert, M. Kiewe, and D. Poznanski. A faint type of supernova from a white dwarf with a helium-rich companion. *Nature*, 465(7296):322–325, May 2010. doi: 10.1038/nature09056.
- Mansi M. Kasliwal, S. R. Kulkarni, Avishay Gal-Yam, Peter E. Nugent, Mark Sullivan, Lars Bildsten, Ofer Yaron, Hagai B. Perets, Iair Arcavi, Sagi Ben-Ami, Varun B. Bhalerao, Joshua S. Bloom, S. Bradley Cenko, Alexei V. Filippenko, Dale A. Frail, Mohan Ganeshalingam, Assaf Horesh, D. Andrew Howell, Nicholas M. Law, Douglas C. Leonard, Weidong Li, Eran O. Ofek, David Polishook, Dovi Poznanski, Robert M. Quimby, Jeffrey M. Silverman, Assaf Sternberg, and Dong Xu. Calcium-rich Gap Transients in the Remote Outskirts of Galaxies. *ApJ*, 755(2):161, August 2012. doi: 10.1088/0004-637X/755/2/161.
- Mohan Ganeshalingam, Weidong Li, Alexei V. Filippenko, Jeffrey M. Silverman, Ryan Chornock, Ryan J. Foley, Thomas Matheson, Robert P. Kirshner, Peter Milne, Mike Calkins, and Ken J. Shen. The Low-velocity, Rapidly Fading Type Ia Supernova 2002es. *ApJ*, 751(2):142, June 2012. doi: 10.1088/0004-637X/751/2/142.
- Christopher J. White, Mansi M. Kasliwal, Peter E. Nugent, Avishay Gal-Yam, D. Andrew Howell, Mark Sullivan, Ariel Goobar, Anthony L. Piro, Joshua S. Bloom, Shrinivas R. Kulkarni, Russ R. Laher, Frank Masci, Eran O. Ofek, Jason Surace, Sagi Ben-Ami, Yi Cao, S. Bradley Cenko, Isobel M. Hook, Jakob Jönsson, Thomas Matheson, Assaf Sternberg, Robert M. Quimby, and Ofer Yaron. Slow-speed Supernovae from the Palomar Transient Factory: Two Channels. *ApJ*, 799(1):52, January 2015. doi: 10.1088/0004-637X/799/1/52.
- Yi Cao, S. R. Kulkarni, Avishay Gal-Yam, S. Papadogiannakis, P. E. Nugent, Frank J. Masci, and Brian D. Bue. SN2002es-like Supernovae from Different Viewing Angles. *ApJ*, 832(1):86, November 2016. doi: 10.3847/0004-637X/832/1/86.
- Subhash Bose, Maximilian D. Stritzinger, Chris Ashall, Eddie Baron, Peter Hoefflich, L. Galbany, W. B. Hoogendam, E. A. M. Jensen, C. S. Kochanek, R. S. Post, A. Reguitti, N. Elias-Rosa, K. Z. Stanek, Peter Lundqvist, Katie Auchetl, Alejandro Clocchiatti, A. Fiore, Claudia P. Gutiérrez, Jason T. Hinkle, Mark E. Huber, T. de Jaeger, Andrea Pastorello, Anna V. Payne, Mark Phillips, Benjamin J. Shappee, and Michael A. Tucker. Expanding the parameter space of 2002es-like type Ia supernovae: on the underluminous ASASSN-20jq / SN 2020qxp. *arXiv e-prints*, art. arXiv:2501.04086, January 2025. doi: 10.48550/arXiv.2501.04086.
- Weidong Li, Alexei V. Filippenko, Ryan Chornock, Edo Berger, Perry Berlind, Michael L. Calkins, Peter Challis, Chris Fassnacht, Saurabh Jha, Robert P. Kirshner, Thomas Matheson, Wallace L. W. Sargent, Robert A. Simcoe, Graeme H. Smith, and Gordon Squires. SN 2002cx: The Most Peculiar Known Type Ia Supernova. *PASP*, 115(806):453–473, April 2003. doi: 10.1086/374200.
- Ryan J. Foley, P. J. Challis, R. Chornock, M. Ganeshalingam, W. Li, G. H. Marion, N. I. Morrell, G. Pignata, M. D. Stritzinger, J. M. Silverman, X. Wang, J. P. Anderson, A. V. Filippenko, W. L. Freedman,

- M. Hamuy, S. W. Jha, R. P. Kirshner, C. McCully, S. E. Persson, M. M. Phillips, D. E. Reichart, and A. M. Soderberg. Type Iax Supernovae: A New Class of Stellar Explosion. *ApJ*, 767(1):57, April 2013. doi: 10.1088/0004-637X/767/1/57.
- Saurabh W. Jha. Type Iax Supernovae. In Athem W. Alsabti and Paul Murdin, editors, *Handbook of Supernovae*, page 375. 2017. doi: 10.1007/978-3-319-21846-5\_42.
- D. K. Sahu, Masaomi Tanaka, G. C. Anupama, Koji S. Kawabata, Keiichi Maeda, Nozomu Tominaga, Ken'ichi Nomoto, Paolo A. Mazzali, and T. P. Prabhu. The Evolution of the Peculiar Type Ia Supernova SN 2005hk over 400 Days. *ApJ*, 680(1):580–592, June 2008. doi: 10.1086/587772.
- Saurabh Jha, David Branch, Ryan Chornock, Ryan J. Foley, Weidong Li, Brandon J. Swift, Darrin Casebeer, and Alexei V. Filippenko. Late-Time Spectroscopy of SN 2002cx: The Prototype of a New Subclass of Type Ia Supernovae. *AJ*, 132(1):189–196, July 2006. doi: 10.1086/504599.
- Ryan J. Foley, Saurabh W. Jha, Yen-Chen Pan, Wei Kang Zheng, Lars Bildsten, Alexei V. Filippenko, and Daniel Kasen. Late-time spectroscopy of Type Iax Supernovae. *MNRAS*, 461(1):433–457, September 2016. doi: 10.1093/mnras/stw1320.
- Yssavo Camacho-Neves, Saurabh W. Jha, Barnabas Barna, Mi Dai, Alexei V. Filippenko, Ryan J. Foley, Griffin Hosseinzadeh, D. Andrew Howell, Joel Johansson, Patrick L. Kelly, Wolfgang E. Kerzendorf, Lindsey A. Kwok, Conor Larison, Mark R. Magee, Curtis McCully, John T. O'Brien, Yen-Chen Pan, Viraj Pandya, Jaladh Singhal, Benjamin E. Stahl, Tamás Szalai, Meredith Wieber, and Marc Williamson. Over 500 Days in the Life of the Photosphere of the Type Iax Supernova SN 2014dt. *ApJ*, 951(1):67, July 2023. doi: 10.3847/1538-4357/acd558.
- Michaela Schwab, Lindsey A. Kwok, Saurabh W. Jha, Curtis McCully, Or Graur, Ryan J. Foley, Yssavo Camacho-Neves, Max J. B. Newman, Conor Larison, and Huei Sears. The Remarkable Late-Time Flux Excess in Hubble Space Telescope Observations of the Type Iax Supernova 2012Z. *arXiv e-prints*, art. arXiv:2504.01063, April 2025. doi: 10.48550/arXiv.2504.01063.
- George C. Jordan, IV, Hagai B. Perets, Robert T. Fisher, and Daniel R. van Rossum. Failed-detonation Supernovae: Subluminous Low-velocity Ia Supernovae and their Kicked Remnant White Dwarfs with Iron-rich Cores. *ApJ*, 761(2):L23, December 2012. doi: 10.1088/2041-8205/761/2/L23.
- M. Kromer, M. Fink, V. Stanishev, S. Taubenberger, F. Ciaraldi-Schoolman, R. Pakmor, F. K. Röpkke, A. J. Ruiter, I. R. Seitenzahl, S. A. Sim, G. Blanc, N. Elias-Rosa, and W. Hillebrandt. 3D deflagration simulations leaving bound remnants: a model for 2002cx-like Type Ia supernovae. *MNRAS*, 429(3):2287–2297, March 2013. doi: 10.1093/mnras/sts498.
- Michael Fink, Markus Kromer, Ivo R. Seitenzahl, Franco Ciaraldi-Schoolmann, Friedrich K. Röpkke, Stuart A. Sim, Rüdiger Pakmor, Ashley J. Ruiter, and Wolfgang Hillebrandt. Three-dimensional pure deflagration models with nucleosynthesis and synthetic observables for Type Ia supernovae. *MNRAS*, 438(2):1762–1783, February 2014. doi: 10.1093/mnras/stt2315.
- Vrutant Mehta, Jack Sullivan, Robert Fisher, Yuken Ohshiro, Hiroya Yamaguchi, Khanak Bhargava, and Sudarshan Neopane. Hydrodynamical simulations favour a pure deflagration origin of the near-chandrasekhar mass supernova remnant 3C 397. *MNRAS*, 532(1):1087–1098, July 2024. doi: 10.1093/mnras/stae1559.
- I. Iben, Jr. and A. V. Tutukov. The evolution of low-mass close binaries influenced by the radiation of gravitational waves and by a magnetic stellar wind. *ApJ*, 284:719–744, September 1984. doi: 10.1086/162455.
- O. Yaron, D. Prialnik, M. M. Shara, and A. Kovetz. An Extended Grid of Nova Models. II. The Parameter Space of Nova Outbursts. *ApJ*, 623(1):398–410, April 2005. doi: 10.1086/428435.
- Sumner Starrfield, Maitrayee Bose, Christian Iliadis, W. Raphael Hix, Charles E. Woodward, and R. Mark Wagner. Carbon-Oxygen Classical Novae Are Galactic  ${}^7\text{Li}$  Producers as well as Potential Supernova Ia Progenitors. *ApJ*, 895(1):70, May 2020. doi: 10.3847/1538-4357/ab8d23.
- Yael Hillman. In-depth analysis of evolving binary systems that produce nova eruptions. *MNRAS*, 505(3):3260–3272, August 2021. doi: 10.1093/mnras/stab1615.
- Yael Hillman, Amir Michaelis, and Hagai B. Perets. Helium Accumulation and Thermonuclear Instabilities on Accreting White Dwarfs: From Recurring Helium Novae to Type Ia Supernovae. *arXiv e-prints*, art. arXiv:2503.12586, March 2025. doi: 10.48550/arXiv.2503.12586.

- Shubham Srivastav, S. J. Smartt, M. E. Huber, K. C. Chambers, C. R. Angus, T. W. Chen, F. P. Callan, J. H. Gillanders, O. R. McBrien, S. A. Sim, M. Fulton, J. Hjorth, K. W. Smith, D. R. Young, K. Auchettl, J. P. Anderson, G. Pignata, T. J. L. de Boer, C. C. Lin, and E. A. Magnier. SN 2020kyg and the rates of faint Iax supernovae from ATLAS. *MNRAS*, 511(2):2708–2731, April 2022. doi: 10.1093/mnras/stac177.
- Ryan J. Foley, Ryan Chornock, Alexei V. Filippenko, Mohan Ganeshalingam, Robert P. Kirshner, Weidong Li, S. Bradley Cenko, Peter J. Challis, Andrew S. Friedman, Maryam Modjaz, Jeffrey M. Silverman, and W. Michael Wood-Vasey. SN 2008ha: An Extremely Low Luminosity and Exceptionally Low Energy Supernova. *AJ*, 138(2):376–391, August 2009. doi: 10.1088/0004-6256/138/2/376.
- M. D. Stritzinger, E. Hsiao, S. Valenti, F. Taddia, T. J. Rivera-Thorsen, G. Leloudas, K. Maeda, A. Pastorello, M. M. Phillips, G. Pignata, E. Baron, C. R. Burns, C. Contreras, G. Folatelli, M. Hamuy, P. Höflich, N. Morrell, J. L. Prieto, S. Benetti, A. Campillay, J. B. Haislip, A. P. LaClutze, J. P. Moore, and D. E. Reichart. Optical and near-IR observations of the faint and fast 2008ha-like supernova 2010ae. *A&A*, 561:A146, January 2014. doi: 10.1051/0004-6361/201322889.
- Masayuki Yamanaka, Keiichi Maeda, Koji S. Kawabata, Masaomi Tanaka, Nozomu Tominaga, Hiroshi Akitaya, Takahiro Nagayama, Daisuke Kuroda, Jun Takahashi, Yoshihiko Saito, Kenshi Yanagisawa, Akihiko Fukui, Ryo Miyanooshita, Makoto Watanabe, Akira Arai, Mizuki Isogai, Takashi Hattori, Hidekazu Hanayama, Ryosuke Itoh, Takahiro Ui, Katsutoshi Takaki, Issei Ueno, Michitoshi Yoshida, Gamal B. Ali, Ahmed Essam, Akihito Ozaki, Hikaru Nakao, Ko Hamamoto, Daisaku Nogami, Tomoki Morokuma, Yumiko Oasa, Hideyuki Izumiura, and Kazuhiro Sekiguchi. OISTER Optical and Near-Infrared Observations of Type Iax Supernova 2012Z. *ApJ*, 806(2):191, June 2015. doi: 10.1088/0004-637X/806/2/191.
- S. Vennes, P. Nemeth, A. Kawka, J. R. Thorstensen, V. Khalack, L. Ferrario, and E. H. Alper. An unusual white dwarf star may be a surviving remnant of a sub-luminous Type Ia supernova. *Science*, 357(6352):680–683, August 2017. doi: 10.1126/science.aam8378.
- K. Nomoto. Accreting white dwarf models for type I supernovae. I - Presupernova evolution and triggering mechanisms. *ApJ*, 253:798–810, February 1982. doi: 10.1086/159682.
- I. Hachisu, M. Kato, and K. Nomoto. A New Model for Progenitor Systems of Type IA Supernovae. *ApJ*, 470:L97, October 1996. doi: 10.1086/310303.
- Y. Hillman, D. Prialnik, A. Kovetz, and M. M. Shara. Growing White Dwarfs to the Chandrasekhar Limit: The Parameter Space of the Single Degenerate SNIa Channel. *ApJ*, 819(2):168, March 2016. doi: 10.3847/0004-637X/819/2/168.
- A. A. Miller, M. M. Kasliwal, Y. Cao, S. M. Adams, A. Goobar, S. Knežević, R. R. Laher, R. Lunnan, F. J. Masci, P. E. Nugent, D. A. Perley, T. Petrushevska, R. M. Quimby, U. D. Rebbapragada, J. Sollerman, F. Taddia, and S. R. Kulkarni. Color Me Intrigued: The Discovery of iPTF 16fmm, an SN 2002cx-like Object. *ApJ*, 848(1):59, October 2017. doi: 10.3847/1538-4357/aa8c7e.
- B. Fryxell, K. Olson, P. Ricker, F. X. Timmes, M. Zingale, D. Q. Lamb, P. MacNeice, R. Rosner, J. W. Truran, and H. Tufo. FLASH: An Adaptive Mesh Hydrodynamics Code for Modeling Astrophysical Thermonuclear Flashes. *ApJS*, 131(1):273–334, November 2000. doi: 10.1086/317361.
- Dongwook Lee. *An unsplit staggered mesh scheme for multidimensional magnetohydrodynamics: A staggered dissipation-control differencing algorithm*. PhD thesis, University of Maryland, College Park, January 2006.
- Dongwook Lee and Anil E. Deane. An unsplit staggered mesh scheme for multidimensional magnetohydrodynamics. *Journal of Computational Physics*, 228(4):952–975, March 2009. doi: 10.1016/j.jcp.2008.08.026.
- Dongwook Lee. A solution accurate, efficient and stable unsplit staggered mesh scheme for three dimensional magnetohydrodynamics. *Journal of Computational Physics*, 243:269–292, June 2013. doi: 10.1016/j.jcp.2013.02.049.
- Josep M. Aparicio. A Simple and Accurate Method for the Calculation of Generalized Fermi Functions. *ApJS*, 117(2):627–632, July 1998. doi: 10.1086/313121.
- F. X. Timmes and Dave Arnett. The Accuracy, Consistency, and Speed of Five Equations of State for Stellar Hydrodynamics. *ApJS*, 125(1):277–294, November 1999. doi: 10.1086/313271.
- F. X. Timmes and F. Douglas Swesty. The Accuracy, Consistency, and Speed of an Electron-Positron Equation of State Based on Table Interpolation of the Helmholtz Free Energy. *ApJS*, 126(2):501–516, February 2000. doi: 10.1086/313304.

A. C. Calder, D. M. Townsley, I. R. Seitenzahl, F. Peng, O. E. B. Messer, N. Vladimirova, E. F. Brown, J. W. Truran, and D. Q. Lamb. Capturing the Fire: Flame Energetics and Neutronization for Type Ia Supernova Simulations. *ApJ*, 656(1):313–332, February 2007. doi: 10.1086/510709.

D. M. Townsley, A. C. Calder, S. M. Asida, I. R. Seitenzahl, F. Peng, N. Vladimirova, D. Q. Lamb, and J. W. Truran. Flame Evolution During Type Ia Supernovae and the Deflagration Phase in the Gravitationally Confined Detonation Scenario. *ApJ*, 668(2):1118–1131, October 2007. doi: 10.1086/521013.

Dean M. Townsley, Aaron P. Jackson, Alan C. Calder, David A. Chamulak, Edward F. Brown, and F. X. Timmes. Evaluating Systematic Dependencies of Type Ia Supernovae: The Influence of Progenitor  $^{22}\text{Ne}$  Content on Dynamics. *ApJ*, 701(2):1582–1604, August 2009. doi: 10.1088/0004-637X/701/2/1582.

Dean M. Townsley, Broxton J. Miles, F. X. Timmes, Alan C. Calder, and Edward F. Brown. A Tracer Method for Computing Type Ia Supernova Yields: Burning Model Calibration, Reconstruction of Thickened Flames, and Verification for Planar Detonations. *ApJS*, 225(1):3, July 2016. doi: 10.3847/0067-0049/225/1/3.